

Transformation of Personal Computers and Mobile Phones into Genetic Diagnostic Systems

Faye M. Walker,^{†,‡} Kareem M. Ahmad,^{‡,§} Michael Eisenstein,^{§,||} and H. Tom Soh^{*,‡,§,||}

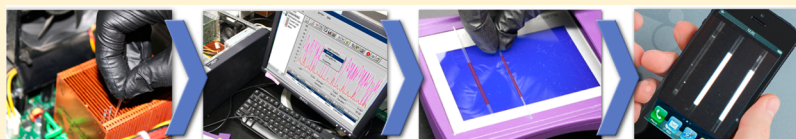
[†]Department of Chemistry and Biochemistry, University of California, Santa Barbara, California 93106, United States

[‡]Interdepartmental Program in Biomolecular Science and Engineering, University of California, Santa Barbara, California 93106, United States

[§]Department of Materials, University of California, Santa Barbara, California 93106, United States

^{||}Department of Mechanical Engineering, University of California, Santa Barbara, California 93106, United States

S Supporting Information



ABSTRACT: Molecular diagnostics based on the polymerase chain reaction (PCR) offer rapid and sensitive means for detecting infectious disease, but prohibitive costs have impeded their use in resource-limited settings where such diseases are endemic. In this work, we report an innovative method for transforming a desktop computer and a mobile camera phone—devices that have become readily accessible in developing countries—into a highly sensitive DNA detection system. This transformation was achieved by converting a desktop computer into a *de facto* thermal cycler with software that controls the temperature of the central processing unit (CPU), allowing for highly efficient PCR. Next, we reconfigured the mobile phone into a fluorescence imager by adding a low-cost filter, which enabled us to quantitatively measure the resulting PCR amplicons. Our system is highly sensitive, achieving quantitative detection of as little as 9.6 attograms of target DNA, and we show that its performance is comparable to advanced laboratory instruments at approximately 1/500th of the cost. Finally, in order to demonstrate clinical utility, we have used our platform for the successful detection of genomic DNA from the parasite that causes Chagas disease, *Trypanosoma cruzi*, directly in whole, unprocessed human blood at concentrations 4-fold below the clinical titer of the parasite.

Although advanced molecular diagnostic technologies for the detection of infectious diseases such as human immunodeficiency virus (HIV), malaria, and tuberculosis^{1,2} are widely available in the developed world, prohibitive costs of equipment and reagents have impeded their adoption in the less developed countries (LDCs) in which these diseases are most prevalent.^{3–6} In contrast, access to certain consumer electronics has surged over the past decade in these same LDCs. For instance, the number of mobile cellular subscribers in the developing world rose by more than 600 million between 2010 and 2011,⁷ and desktop computer penetration has dramatically accelerated since the start of the millenium.⁸

This trend offers an exciting opportunity for leveraging such tools as a means to affordably improve healthcare. For example, the built-in cameras in mobile phones have been adapted as imaging platforms^{9,10} for detecting disease biomarkers and infectious pathogens^{11–16} in blood and other clinically relevant samples.^{17–20} However, as these methods are microscopy-based, they can suffer from poor limits of detection and the challenge of differentiating among similar species, subspecies, and strains.²¹ Nucleic acid-based genetic tests offer higher sensitivity and exquisite specificity,^{22,23} and several innovative approaches have been explored to develop low-cost assays and instruments for genetic detection at the point-of-care. For

example, Manage et al. achieved streamlined detection of BK viruses by performing polymerase chain reaction (PCR) directly in whole blood using self-contained gel strips.²⁴ In addition, several groups have demonstrated “sample-in-answer-out” systems that integrate multiple process steps into a monolithic device using microfluidics technology.^{25–28} The Landers group pioneered the use of microfluidics for genetic analysis,²⁹ isolating and amplifying nucleic acids directly from buccal swabs and whole blood for clinical examination.³⁰ Our group has similarly demonstrated direct detection of H1N1 influenza viruses in throat swab samples by integrating magnetic separation with reverse transcriptase PCR (RT-PCR) in a disposable device.³¹ In practice, however, the deployment of these systems in low-resource settings is challenging because they often rely on specialized devices and instrumentation (e.g., pumps, syringes, and detectors) that have limited availability and require skilled technicians for operation.

We have developed an alternate approach to molecular diagnostics that largely eliminates the need for such apparatuses. Instead of relying on custom-built machines, we

Received: June 18, 2014

Accepted: August 6, 2014

Published: August 31, 2014

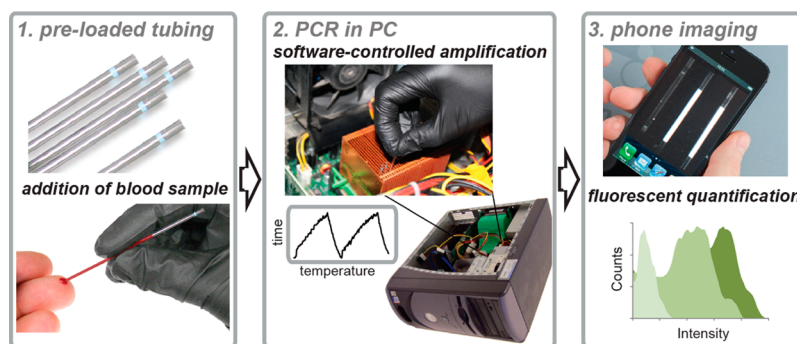


Figure 1. P3 assay schematic. First, a small drop of blood obtained via finger prick is added to a length of preloaded capillary tubing containing the reagents required for PCR. The tubing is then inserted between the cooling fins on the heat sink in the computer. Commercial software controls CPU usage, cyclically heating and cooling the computer according to a protocol designed to amplify target DNA. After thermal cycling, the samples are exposed to UV light and imaged with a camera phone. By comparing a histogram of the pixel intensities for the patient sample relative to control samples, the presence or absence of target pathogenic DNA can be determined.

repurpose a desktop PC and a mobile camera phone into a highly sensitive platform for genetic detection of pathogens. Specifically, we use low-cost software tools to convert the PC into a *de facto* thermal cycler for PCR and configure mobile phones as imagers to detect and quantify the resulting PCR amplicons. To our knowledge, this is the first work to perform PCR reactions using a PC. In our PC-PCR-Phone (P3) system, a small volume of patient blood is added directly to a length of disposable tubing that has been preloaded with PCR reagents (Figure 1, step 1). The tubing is then placed into the heat sink of the central processing unit (CPU), where PCR is performed by using two software programs to precisely manipulate the PC's internal temperature (Figure 1, step 2). Subsequently, we use a mobile phone camera to image the amplified products, which are quantified according to their fluorescence intensity (Figure 1, step 3). As a model, we used our P3 system to detect genomic DNA (gDNA) from *Trypanosoma cruzi* (*T. cruzi*), the parasitic protist responsible for Chagas disease,^{32,33} which affects over 17 million people worldwide.^{34,35} We demonstrate direct detection from blood with a limit of detection of 0.1 fg/ μ L, which is well below the average parasitic loads found in clinical samples (0.4 fg/ μ L).

MATERIALS AND METHODS

General Information. All synthetic DNA sequences were purchased from Integrated DNA Technologies (IDT). Hot-start polymerase master mix and nuclease-free water were purchased from Promega. PCR validation was performed with a 100-nt single-stranded DNA sequence reported previously as Thr-02,³⁶ using primers AGCAGCACAGAGGTCAGATG and TTACGGTAGCACGCATAGG. DMSO was obtained from the American Type Culture Collection and used at the concentration indicated. SYBR Green I was obtained from Life Technologies and used at 0.625 \times concentration, and EvaGreen was obtained from Biotium and used at 1 \times concentration. Whole blood preserved in EDTA was obtained from Bioreclamation. Hemo KlenTaq (HKT) polymerase and 5 \times buffer were obtained from New England Biolabs and used in the manufacturer recommended amount. Melting temperatures were measured via the iQ5 real-time multicolor detection system (Bio-Rad).

PC-Based PCR. For initial validation experiments, we used 2 fmol of 100-nt template, with 1 μ M primer in a 50 μ L reaction that included PCR mix (containing DNA polymerase, dNTPs, buffer), EvaGreen, primers, and 13% DMSO. The optimal

DMSO concentration was determined prior to carrying out PCR in a PC by testing the effect of DMSO on dsDNA hybridization in the reaction mixture described above. Melting temperatures were determined by performing 40 cycles of two-step PCR on the 100-nt template to generate double-stranded products in the iQ5. Post-amplification, we carried out a thermal gradient beginning at 65 $^{\circ}$ C and increasing to 85 $^{\circ}$ C at a rate of 1 $^{\circ}$ C per minute and dwell time of 10 s, with fluorescence intensity measured every minute. We then calculated the negative first derivative of the plot of the resulting melting profile of intensity versus temperature. The melting temperature is where this differential plot reaches a maximum, as calculated by Bio-Rad iQ5 melt curve analysis (Supplemental Figure 2, Supporting Information). To perform PC-based PCR, the reaction mixture was preloaded into short capillaries of perfluoroalkoxyl (PFA) tubing. After adding template at a concentration of 40 fg/ μ L, the capillary tubes were permanently sealed at both ends by epoxy (Devcon) to yield contaminant-free testers that are amenable to high-throughput manufacturing. The capillary tube was then inserted between the CPU heat sink fins of a Dell Pentium 4 desktop computer for cycling.

For measuring the actual temperature of the sample, we used a digital thermometer (Fluke) and K type thermocouple (Omega). Thermal measurements were performed by recording the solution temperature inside the capillaries with 50 μ L of distilled water using a thermocouple probe. We used two programs to automate the PCR thermocycling process with the computer. The heating of the CPU was achieved with BurnInTest software (Passmark), while SpeedFan (Almico) program obtained the CPU temperature from the built-in thermocouples and controlled the fan for cooling.

The resulting PCR product was loaded and run on 10% TBE polyacrylamide gels (Bio-Rad) with a 20 bp DNA ladder (Bio-Rad) in 4 $^{\circ}$ C running buffer. After 15 min of gel electrophoresis at 300 V, the gels were stained with Gelstar (Lonza) for 10 min. The stained gels were imaged on a Gel Logic System using UV transillumination and a 535 nm optical filter (Kodak). The positive control PCR was performed by taking an aliquot of the same sample and carrying out amplification in a commercial thermal cycler using 0.2 mL capped tubes (Bio-Rad). In both the PC and cycler, the template was amplified for no more than 20 cycles. This number was calculated to be the appropriate threshold cycle (C_t) based on real-time quantitative PCR using a Bio-Rad iQ5.

Genomic DNA from *T. cruzi* (Tulahuen strain) was obtained from ATCC. The sequence for the Diaz primer set was CGCAAACAGATATTGACAGA and TGTTCACACACTGGACACCAA,³⁸ which target the 195-bp repetitive element in *T. cruzi* nuclear DNA. Capillaries were prepped with 20 μ L of reaction mixture containing HK Taq polymerase, 0.2 mM dNTPs, 1 \times buffer, SYBR Green I, 0.2 μ M primers, and 13% DMSO. Spiked human whole blood containing gDNA (or blood itself in the case of the negative control) was added to a final concentration of 5% (v/v) by pipetting the blood into the tubing and allowing it to settle at the bottom of the buffer layer without any vigorous mixing.³⁷ Next, 1 μ L of human blood was loaded into the capillaries, and the capillary tubes were sealed on both ends and heated in a boiling water bath for 2 min to simulate cell lysis and gDNA denaturation steps prior to PC-PCR amplification. From an initial annealing/extension temperature of 64.5 $^{\circ}$ C, the annealing/extension step was reduced by a difference of 3 $^{\circ}$ C every three cycles for the initial step-down cycling phase. After 15 cycles, we maintained the annealing temperature at 49.5 $^{\circ}$ C for 40 cycles to complete the amplification phase of SD-PCR (Supplemental Figure S5, Supporting Information).

Post-PCR Imaging. Initial characterization of the camera phone's (Samsung Galaxy S) fluorescent imaging capabilities was performed with EvaGreen dye, and the PCR products were generated from the Thr-02 template after 30 cycles of PCR in a standard thermal cycler (Bio-Rad). Real-time quantitative PCR in a Bio-Rad iQ5 was used to determine that 30 cycles was the upper threshold for efficient amplification of a single PCR product from this template. Further applications with SYBR Green I stain and *T. cruzi* gDNA in whole blood were performed according to the SD-PCR protocol described in the section above. Samples were excited by a UV transilluminator (Kodak). For imaging, a 520 ± 10 nm bandpass filter (Edmund Optics) was placed over the mobile phone camera and held in place by a silicone case. The phone was situated at fixed distance above the samples, and the image was captured using the "night mode" option on the camera phone. Images were transferred to a computer and analyzed with ImageJ software (<http://www.nih.gov/>). Rectangular regions of interest were drawn around each sample, and the histogram of pixel intensities was obtained. Mean histogram values of all samples were then background-subtracted with the mean histogram value of an empty tube. Average and standard deviations are the result of at least four individual trial runs. Data were imported into MATLAB and plotted. For relative image analysis, the `imsubtract` function in MATLAB was used to subtract each element in a sample image by the same element in the blank (empty) image. From the resulting RGB values, background-subtracted images were graphed using the `imshow` function.

RESULTS AND DISCUSSION

Efficient Amplification of Genomic DNA in Blood Using a PC. PCR amplification of genomic DNA (gDNA) in blood can be hindered by the presence of enzymatic inhibitors naturally found in blood or anticoagulants added after sample collection.³⁹ To circumvent this problem, we implemented three key modifications to the standard PCR protocol⁴⁰ (see Materials and Methods). First, we used a step-down (SD)-PCR⁴¹ approach that enables specific and high-yield amplification of long template DNA (i.e., gDNA) with reduced byproducts.⁴² Second, we adopted a two-temperature PCR scheme, consisting of a hot start followed by alternating

hybridization/extension and denaturation steps, simplifying accurate feedback control of the CPU temperature.

To complete the modified PCR protocol associated with our system, we reduced the denaturation temperature to below the maximum temperature for safe, extended CPU operation (90 $^{\circ}$ C). We achieved this by adding dimethyl sulfoxide (DMSO) to our PCR mixture, which decreased the melting temperature (T_m) of our primer-template duplex by -0.6 $^{\circ}$ C per 1% DMSO (Supplemental Figure S1, Supporting Information). As an added benefit, the addition of DMSO also improves yield and further reduces undesired byproducts.^{43,44}

Software-Based Thermal Cycling in a PC. We installed two software programs that can effectively convert a desktop PC into a PCR thermal cycler. The first program (BurnIn Test) is used to rapidly increase the CPU temperature through intensive computational operations. The second program (SpeedFan) measures the temperature of the CPU in real-time using the built-in thermal sensors common to all CPUs and also controls the cooling fan. By running these two programs, the surface temperature of the CPU can be precisely regulated under automated control (Figure 2a, black trace). However, due to thermal resistance between the heat sink and tubing (even in the presence of interfacing compounds such as

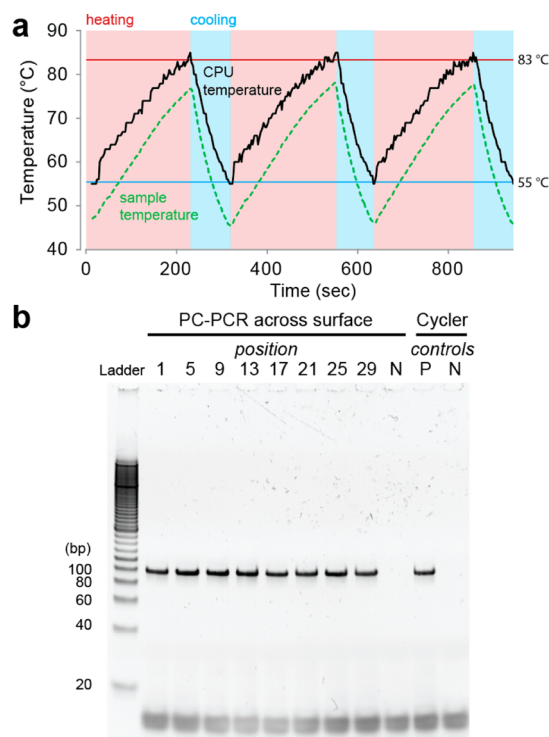


Figure 2. DNA amplification achieved via robust thermal cycling within the PC heat sink. (a) Temperature traces of the reported CPU temperature (black trace) as recorded by SpeedFan software compared with the measured sample temperature (green trace) as obtained by a thermocouple probe over the course of three cycles. Each two-step PCR cycle started at a temperature of 55 $^{\circ}$ C for annealing and extension, which was then raised to 83 $^{\circ}$ C for melting. The vertical bars indicate when the CPU (heating, red bars) and fans (cooling, blue bars) were active. (b) PAGE image showing amplification of a synthetic 100-nt template from reactions performed within the PC heat sink. Control reactions were performed by carrying out 20 cycles of PCR on aliquots of the same negative and positive samples in a commercial thermal cycler.

thermal paste), the temperature of the blood sample is lower than that of the CPU. In order to correct for this difference, we measured the actual temperature of the sample using thermocouples (Figure 2a, green trace). These data indicate that the difference in temperature between the CPU and sample does not vary by more than several degrees and can be accurately predicted with a calibration curve. We established a linear correlation with excellent fit ($R^2 = 0.992$ for heating and 0.995 for cooling, Supplemental Figure S2, Supporting Information) to account for the effect of thermal resistance. Since this thermal resistance should not vary across models of PC, we believe our calibration curve can be used generally and that it is not necessary to calibrate each PC individually.

PC-PCR Produces Single-Length Amplicons with High Yield. Our system is capable of simultaneously performing PCR on up to 29 samples with reproducible yield and no spurious byproducts. To verify that our PCR protocol only generates amplicons of the predicted 100-nt length, we prepared 10 identical samples (20 μL each) and monitored the reaction at every other PCR cycle. Visualization with polyacrylamide gel electrophoresis (PAGE) clearly showed a single product band that matched positive control amplicons obtained with a conventional laboratory thermal cycler (Supplemental Figure S3, Supporting Information). We subsequently tested the capacity of our system by performing PCR on 29 identical reactions distributed across the CPU heat sink. We observed minimal variability in amplification (Figure 2b), both among the various CPU samples and relative to a control amplification performed in a laboratory thermal cycler, as measured by image densitometry following PAGE (C.V. < 4%).

Optical DNA Detection with a Camera Phone. In order to achieve convenient and quantitative means of readout after amplification, we repurposed a standard camera phone into a quantitative DNA detection platform capable of measuring as little as 9.6 ag of template DNA. Specifically, we outfitted the camera phone with a monochromatic filter to capture fluorescence from a DNA binding dye (see Materials and Methods). This dye is present in the PCR mix prior to the reaction and emits green light (peak wavelength = 520 nm) under UV excitation when complexed with double-stranded DNA amplicons. Using this setup, we were able to clearly differentiate fluorescent signals obtained from PCR reactions performed in a conventional thermal cycler with samples containing as little as 9.6 ag of template DNA relative to a template-free negative control (Figure 3a). Moreover, the detection performance of our camera phone system is comparable to that of a laboratory real-time quantitative PCR (qPCR) instrument. Software analysis yielded normalized, mean fluorescence intensity values of our camera phone images (see Materials and Methods), which we plotted as a function of template copy number (Figure 3b, black). We compared these results with the normalized end-point fluorescence values obtained from a qPCR instrument (Bio-Rad iQ5) (Figure 3b, red). We found that the respective performance of these two platforms correlates very closely, with an $R^2 > 0.99$ (Supplemental Figure S4, Supporting Information), and falls within each other's error range at low template values (<153 ag).

Detection of *T. cruzi* Using the P3 System. The average concentration of *T. cruzi* gDNA in blood samples of patients infected with Chagas disease is 0.4 fg/ μL .⁴⁵ We found that our P3 system can attain sensitivities below this level from

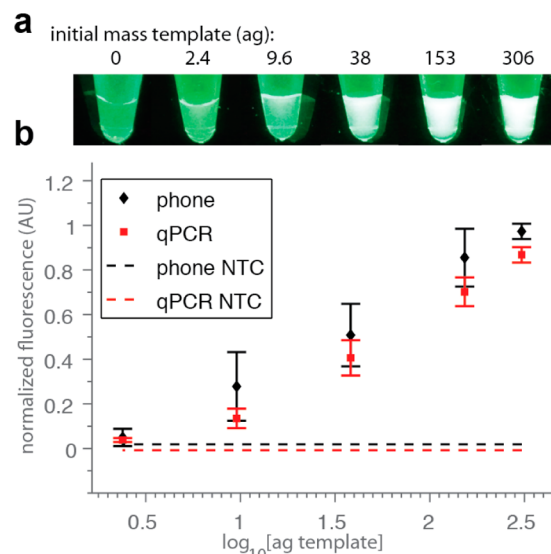


Figure 3. Validation of DNA amplicon detection using a mobile phone camera. (a) Samples containing a range of template molecules were amplified for 30 cycles with EvaGreen, excited by UV transillumination, and imaged with a mobile phone camera and 520 nm filter. (b) Sensitivity and specificity of camera phone detection of amplified DNA in comparison to qPCR end-point detection. The normalized fluorescence for 10 independent experiments is plotted versus the log of the initial template mass.

unprocessed whole blood samples. We performed P3 analysis on 20 μL samples containing 1 μL of whole blood that had been spiked with 0, 0.1, 1, 10, or 100 fg of *T. cruzi* gDNA. After subtracting the background fluorescence from an empty capillary tube, we could clearly distinguish reactions that had been performed with as little as 0.1 fg/ μL gDNA from negative controls (Figure 4a). PAGE analysis confirmed that the amplicons detected by the P3 system were the predicted 195-bp satellite repeat specific to the Diaz1/Diaz2 primer set⁴⁶ and that the PCR performance is comparable to that of a laboratory thermal cycler instrument (Figure 4b). These data suggest that our P3 system should be capable of detecting clinically relevant concentrations of *T. cruzi* gDNA directly from the blood of patients infected with Chagas disease.

CONCLUSIONS

In this work, we report the feasibility of transforming a desktop computer and cell phone into a molecular diagnostic system capable of highly sensitive and quantitative pathogen DNA detection. These devices are becoming increasingly available in developing countries, especially with the aid of humanitarian organizations dedicated to expanding the reach of technology in areas of need.^{47,48} Using two programs, one free and the other affordably priced, we are able to convert a PC into a highly responsive thermal cycler; by adding a simple filter, we are likewise able to use a standard camera phone for the quantitative optical detection of PCR amplicons. We showed that the P3 system is capable of achieving sensitivities and specificities comparable to that of conventional laboratory instruments at 1/500th of the cost (Supplemental Table S1, Supporting Information). In an initial demonstration with the Chagas disease pathogen *T. cruzi*, we achieved a limit of detection for gDNA that is 4-fold below the average clinical concentration typically found in patients. There are a number of advantageous features inherent to the P3 system. First,

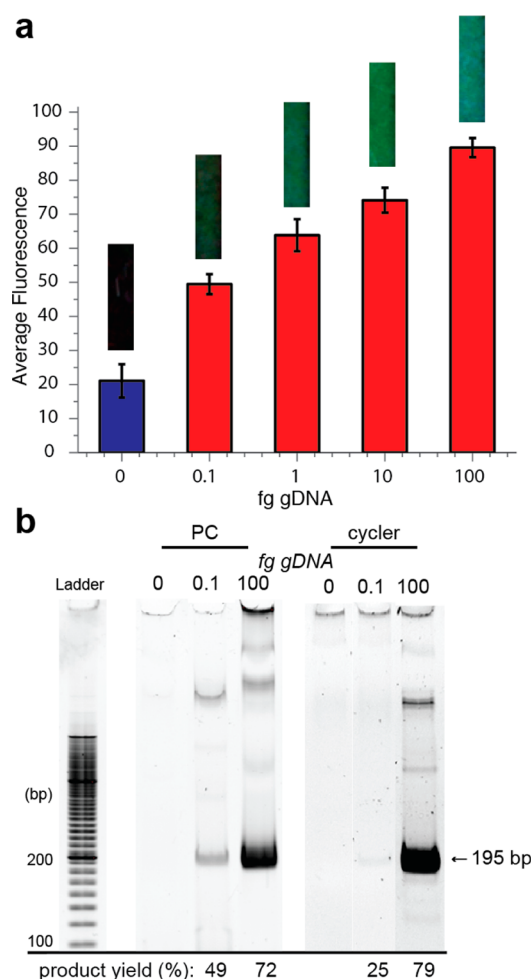


Figure 4. Detection of *T. cruzi* gDNA in whole blood. (a) Images of capillary tubing positioned above bar graphs depict the fluorescence signal obtained from each amount of template gDNA after background subtraction. P3 is sufficiently sensitive to reproducibly detect 0.1 fg of gDNA in 1 μ L of whole blood. Error bars were obtained from 4 replicates. (b) Gel analysis shows the specific amplification of a 195-nt region of tandemly repeating gDNA. A side-by-side comparison of the same sample after PCR carried out in a PC or a laboratory thermal cycler shows that PC-PCR can match the efficiency of laboratory instrumentation.

sample prep and handling is minimal, as our assay is performed directly in blood with no need for mechanical or chemical processing and only a brief boiling step required as a prelude to PCR. Additionally, P3 greatly reduces the potential for cross-contamination through the use of a single, sealed capillary tube. Finally, our system allows multiple samples to be analyzed at once (up to 29 in the current configuration), and we envision that it can be adopted for multiplexed detection of multiple pathogens in separate capillaries.

The sensor technology presented here represents a rapid and facile means of pathogen detection in low-resource settings, as indicated by the detection of gDNA in blood. In its current iteration, we anticipate that P3 will work primarily as a binary diagnostic assay in which an end point sample readout is compared to positive and negative controls to determine the presence of pathogenic infection. Though beyond the scope of this work, we envision that future iterations of the system will demonstrate equivalent performance with patient blood samples containing intact parasites. Several examples in the

literature have already established precedents for successful PCR-based detection in blood samples without DNA extraction directly from pathogens such as parasites⁴⁹ and viruses,⁵⁰ as well as trypanosomes.⁵¹ We are therefore confident that P3 can achieve a similar level of performance with minimal modifications through techniques such as heat pretreatment and optimization of buffers to facilitate the release of gDNA from lysed pathogens. Finally, we are currently investigating the potential for adapting P3 for use in more remote regions. As resource-limited settings may not have access to reliable power sources for refrigeration or computational operation, lyophilized reagents²² and battery-powered laptops could be implemented in future iterations. Laptop CPUs have the added advantage of functioning at even higher temperatures than desktop computers with increased portability. Similarly, low-cost blue LEDs and a blacked-out cardboard box can replace UV transilluminators while blocking ambient light for a more inexpensive method of dye excitation (peak absorption wavelength = 500 nm). In sum, we report an innovative method for transforming widely available consumer electronics into tools for molecular biotechnology. We believe such repurposing may offer versatile strategies for providing molecular diagnostic capabilities to resource-limited settings in a cost-effective manner for a diverse spectrum of diseases.

■ ASSOCIATED CONTENT

Supporting Information

Additional information as noted in text. This material is available free of charge via the Internet at <http://pubs.acs.org>.

■ AUTHOR INFORMATION

Corresponding Author

*E-mail: tsoh@engineering.ucsb.edu.

Author Contributions

#F.M.W. and K.M.A. contributed equally.

Notes

The authors declare no competing financial interest.

■ ACKNOWLEDGMENTS

We are grateful for the financial support of the Garland Initiative, ARO Institute for Collaborative Biotechnologies (W911F-09-D-0001), National Institutes of Health (R01A1076899), and Department of Defense (W81XWH-09-0698). The authors would like to thank Peter Allen for his aid with the schematics.

■ REFERENCES

- (1) Tang, Y. W.; Procop, G. W.; Persing, D. H. *Clin. Chem.* **1997**, *43*, 2021–2038.
- (2) Yang, S.; Rothman, R. E. *Lancet* **2004**, *4*, 337–348.
- (3) Fu, B. E.; Yager, P.; Floriano, P. N.; Christodoulides, N.; Mcdevitt, J. T. *IEEE Pulse* **2011**, *2*, 40–50.
- (4) Mabey, D.; Peeling, R. W.; Ustianowski, A.; Perkins, M. D. *Nat. Rev. Microbiol.* **2004**, *2*, 231–240.
- (5) Mathers, C. D.; Ezzati, M.; Lopez, A. D. *PLoS Neglected Trop. Dis.* **2007**, *1*, No. e114.
- (6) Yager, P.; Domingo, G. J.; Gerdes, J. *Annu. Rev. Biomed. Eng.* **2008**, *10*, 107–144.
- (7) Ki-moon, B. *Information Economy Report 2012*; United Nations: Geneva, 2012; http://www.itu.int/dms_pub/itu-d/opb/ind/D-IND-ICTOI-2012-SUM-PDF-E.pdf.
- (8) International Telecommunication Union. *ICT and Telecommunications in Least Developed Countries: Mid-Term Review for the Decade*

2001-2010; ITU: Geneva, 2006; http://www.itu.int/ITU-D/ldc/pdf/ictand_telindlc-e.pdf.

(9) Stedtfeld, R. D.; Tourlousse, D. M.; Seyrig, G.; Stedtfeld, T. M.; Kronlein, M.; Price, S.; Ahmad, F.; Gulari, E.; Tiedje, J. M.; Hashsham, S. A. *Lab Chip* **2012**, *12*, 1454–1462.

(10) Lee, D.; Chou, W. P.; Yeh, S. H.; Chen, P. J.; Chen, P. H. *Biosens. Bioelectron.* **2011**, *26*, 4349–4354.

(11) Preechaburana, P.; Gonzalez, M. C.; Suska, A.; Filippini, D. *Angew. Chem.* **2012**, *124*, 11753–11756.

(12) Wei, Q.; Qi, H.; Luo, W.; Tseng, D.; Ki, S. J.; Wan, Z.; Göröcs, Z.; Bentolila, L. A.; Wu, T.-T.; Sun, R.; Ozcan, A. *ACS Nano* **2013**, *7*, 9147–9155.

(13) Zhu, H.; Sikora, U.; Ozcan, A. *Analyst* **2012**, *137*, 2541–2544.

(14) Greenbaum, A.; Luo, W.; Su, T.-W.; Göröcs, Z.; Xue, L.; Isikman, S. O.; Coskun, A. F.; Mudanyali, O.; Ozcan, A. *Nat. Methods* **2012**, *9*, 889–895.

(15) Balsam, J.; Rasooly, R.; Bruck, H. A.; Rasooly, A. *Biosens. Bioelectron.* **2013**, *51C*, 1–7.

(16) Tseng, D.; Mudanyali, O.; Oztoprak, C.; Isikman, S. O.; Sencan, I.; Yaglidere, O.; Ozcan, A. *Lab Chip* **2010**, *10*, 1787–1792.

(17) Zhu, H.; Mavandadi, S.; Coskun, A. F.; Yaglidere, O.; Ozcan, A. *Anal. Chem.* **2011**, *83*, 6641–6647.

(18) Zhu, H.; Yaglidere, O.; Su, T.-W.; Tseng, D.; Ozcan, A. *Lab Chip* **2011**, *11*, 315–322.

(19) Breslauer, D. N.; Maamari, R. N.; Switz, N. A.; Lam, W. A.; Fletcher, D. A. *PLoS One* **2009**, *4*, No. e6320.

(20) Xie, H.; Mire, J.; Kong, Y.; Chang, M.; Hassounah, H. A.; Thornton, C. N.; Sacchetti, J. C.; Cirillo, J. D.; Rao, J. *Nat. Chem.* **2012**, *4*, 802–809.

(21) Gomes, Y. M.; Lorena, V. M. B.; Luquetti, A. O. *Mem. Inst. Oswaldo Cruz* **2009**, *104* (Suppl), 115–121.

(22) Niemz, A.; Ferguson, T. M.; Boyle, D. S. *Trends Biotechnol.* **2011**, *29*, 240–250.

(23) Carolina, J. D. *Air Water Borne Dis.* **2013**, *02*, 1–10.

(24) Manage, D. P.; Lauzon, J.; Atrazhev, A.; Pang, X.; Pilarski, L. M. *Lab Chip* **2013**, *13*, 4011–4014.

(25) Liu, R. H.; Yang, J.; Lenigk, R.; Bonanno, J.; Grodzinski, P. *Anal. Chem.* **2004**, *76*, 1824–1831.

(26) Chin, C. D.; Laksanasopin, T.; Cheung, Y. K.; Steinmiller, D.; Linder, V.; Parsa, H.; Wang, J.; Moore, H.; Rouse, R.; Umvilighozo, G.; Karita, E.; Mwambarangwe, L.; Braunstein, S. L.; van de Wijgert, J.; Sahabo, R.; Justman, J. E.; El-Sadr, W.; Sia, S. K. *Nat. Med.* **2011**, *17*, 1015–1019.

(27) Martinez, A. W.; Phillips, S. T.; Carrilho, E.; Thomas, S. W.; Sindi, H.; Whitesides, G. M. *Anal. Chem.* **2008**, *80*, 3699–3707.

(28) Foudeh, A. M.; Fatanat Didar, T.; Veres, T.; Tabrizian, M. *Lab Chip* **2012**, *12*, 3249–3266.

(29) Easley, C. J.; Karlinsey, J. M.; Bienvenue, J. M.; Legendre, L. A.; Roper, M. G.; Feldman, S. H.; Hughes, M. A.; Hewlett, E. L.; Merkel, T. J.; Ferrance, J. P.; Landers, J. P. *Proc. Natl. Acad. Sci. U. S. A.* **2006**, *103*, 19272–19277.

(30) Lounsbury, J. A.; Karlsson, A.; Miranian, D. C.; Cronk, S. M.; Nelson, D. A.; Li, J.; Haverstick, D. M.; Kinnon, P.; Saul, D. J.; Landers, J. P. *Lab Chip* **2013**, *13*, 1384–1393.

(31) Ferguson, B. S.; Buchsbaum, S. F.; Wu, T.-T.; Hsieh, K.; Xiao, Y.; Sun, R.; Soh, H. T. *J. Am. Chem. Soc.* **2011**, *133*, 9129–9135.

(32) Rassi, A.; Marin-Neto, J. A. *Lancet* **2010**, *375*, 1388–1402.

(33) Hotez, P. J.; Dumonteil, E.; Woc-Colburn, L.; Serpa, J. A.; Bezek, S.; Edwards, M. S.; Hallmark, C. J.; Musselwhite, L. W.; Flink, B. J.; Bottazzi, M. E. *PLoS Neglected Trop. Dis.* **2012**, *6*, No. e1498.

(34) Martins-Melo, F. R.; Alencar, C. H.; Ramos, A. N.; Heukelbach, J. *PLoS Neglected Trop. Dis.* **2012**, *6*, No. e1508.

(35) Moncayo, A.; Silveira, A. C. *Mem. Inst. Oswaldo Cruz* **2009**, *104* (Suppl), 17–30.

(36) Ahmad, K. M.; Oh, S. S.; Kim, S.; McClellan, F. M.; Xiao, Y.; Soh, H. T. *PLoS One* **2011**, *6*, No. e27051.

(37) Kermekchiev, M. B.; Barnes, W. M. *Use of whole blood in PCR reactions*. U.S. Patent 8470563, 2013.

(38) Diaz, C.; Nussenzweig, V.; Gonzalez, A. *Am. J. Trop. Med. Hyg.* **1992**, *46*, 616–623.

(39) Al-soud, W. A.; Rådström, P. *J. Clin. Microbiol.* **2001**, *39*, 485–493.

(40) Mullis, K.; Faloona, F.; Scharf, S.; Saiki, R.; Horn, G.; Erlich, H. *Cold Spring Harbor Symp. Quant. Biol.* **1986**, *L1*, 263–273.

(41) Hecker, K. H.; Roux, K. H. *Biotechniques* **1996**, *20*, 478–485.

(42) Korbie, D. J.; Mattick, J. S. *Nat. Protoc.* **2008**, *3*, 1452–1456.

(43) Varadaraj, K.; Skinner, D. M. *Gene* **1994**, *140*, 1–5.

(44) Von Ahlsen, N.; Wittwer, C. T.; Schütz, E. *Clin. Chem.* **2001**, *47*, 1956–1961.

(45) Moreira, O. C.; Ramírez, J. D.; Velázquez, E.; Melo, M. F. A. D.; Lima-Ferreira, C.; Guhl, F.; Sosa-Estani, S.; Marin-Neto, J. A.; Morillo, C. A.; Britto, C. *Acta Trop.* **2013**, *125*, 23–31.

(46) Virreira, M.; Torrico, F.; Truyens, C.; Alonso-Vega, C.; Solano, M.; Carlier, Y.; Svoboda, M. *Am. J. Trop. Med. Hyg.* **2003**, *68*, 574–582.

(47) Cristia, J. P.; Ibararán, P.; Cueto, S.; Santiago, A.; Severín, E. *Technology and Child Development: Evidence from the One Laptop Per Child Program*; IZA Discussion Paper No. 6401; IZA: Bonn, Germany, 2012.

(48) Sheriff, R. E., Ed. *Electronics and Telecommunications Research Seminar Series: 10th Workshop Proceedings*; School of Engineering, Design and Technology, University of Bradford: Bradford, UK, 2011.

(49) Li, Y.; Kumar, N.; Gopalakrishnan, A.; Ginocchio, C.; Manji, R.; Bythrow, M.; Lemieux, B.; Kong, H. *J. Mol. Diagn.* **2013**, *15*, 634–641.

(50) Zhang, Z.; Kermekchiev, M. B.; Barnes, W. M. *J. Mol. Diagn.* **2010**, *12*, 152–161.

(51) Ravindran, R.; Rao, J. R.; Mishra, A. K.; Pathak, K. M. L.; Babu, N.; Satheesh, C. C.; Rahul, S. *Vet. Arh.* **2008**, *78*, 89–94.